Available online at www.sciencedirect.com
ScienceDirect
Cement & Concrete Composites 29 (2007) 760–769
Cement & Concrete Composites
www.elsevier.com/locate/cemconcomp

Effect of variations in the plate modulus of elasticity on the failure modes of FRP plated R.C. beams

Mahmoud Hassanen [a,*], M. Raoof [b]

[a] Department of Civil Engineering, University of Strathclyde, John Anderson Building, Glasgow G4 0NG, United Kingdom
[b] Department of Civil and Building Engineering, Loughborough University, Loughborough, Leicestershire LE11 3TU, United Kingdom

Received 19 December 2005; received in revised form 24 May 2007; accepted 25 May 2007
Available online 9 June 2007

Abstract

In the absence of FRP plate/glue/concrete interface bond failure (i.e. interfacial debonding), eight possible flexural modes of failure are identified for reinforced concrete beams experiencing lateral loading, and strengthened in flexure with external FRP or steel plates glued to their soffits. All possible changes in such modes of failure, as a result of variations in the modulus of elasticity of the FRP material (assuming an associated constant value of ultimate tensile strength for the FRP plate in a given beam design), have been addressed in some detail, with a quantitative treatment of the critical values of the FRP modulus of elasticity associated with various failure mode transitions (i.e. changes).

Keywords: Reinforced concrete; External plating; FRP; Flexure; Upgrading; Modes of failure; Modulus of elasticity

1. Introduction

During the 1960s and 1970s, the quality of fibre reinforced plastic (FRP) materials was improved considerably, while the material costs decreased as the manufacturing methods became more automated. However, FRP materials were not used to externally reinforce concrete elements until the late 1980s. Unlike steel, FRP materials can be manufactured to provide a wide range of material characteristics: the ranges of ultimate tensile strength and/or the modulus of elasticity for FRP materials are much wider than the corresponding ones for steel [1]. As regards upgrading of reinforced concrete (R.C.) beams with FRP plates, considerable variations in the behaviour of FRP plated R.C. beams are, then, to be expected as a result of significant changes in the FRP material characteristics [2].

Composite systems of reinforced concrete and FRP sheets have been used to upgrade a wide variety of structural elements including beams, columns, slabs, walls and retaining tanks [3]. Externally bonded FRP plates can be used to increase the load bearing capacity in order to meet the new demands placed on structures due to functional changes, additional loads, or changes in the codes of practice. FRP materials may also be used to provide passive confinement in order to improve seismic resistance, to control cracking or to strengthen critical areas around new openings in, say, slabs. In addition to FRP's relative ease of application and very good resistance to corrosion, external strengthening using FRP sheets yields minor changes in element dimensions which, in certain cases, is a key requirement to ensure that the strengthening procedure is not going to adversely affect any of the structure's original functionalities including dimensions/appearance. In general, upgrading reinforced concrete beams with external FRP plates glued to their soffits can lead to increases in flexural capacity and overall bending stiffness (e.g. [1,3]). However, despite worldwide research on the various characteristics of FRP plated R.C. beams over the last two decades, a generally accepted method to predict the failure load of FRP plated beams is not yet available (e.g. [4–6]).

* Corresponding author. Tel.: +44 141548 3010; fax: +44 141 5532066.
E-mail addresses: Mahmoud.Hassanen@Strath.ac.uk (M. Hassanen), M.Raoof@Lboro.ac.uk (M. Raoof).

0958-9465/$ - see front matter © 2007 Elsevier Ltd. All rights reserved.
doi:10.1016/j.cemconcomp.2007.05.010

There is insufficient space here to attempt a comprehensive literature study, nor does one seem particularly worthwhile when others (e.g. [3,5,7,8]) have made such surveys recently. Very briefly, it is now well-established that depending on the design, an FRP plated beam can exhibit various modes of failure. For some failure modes, such as crushing of the compressive concrete or fracturing of the FRP plate, it is now accepted that the failure load can be predicted by using an analysis similar to that for conventional reinforced concrete members (e.g. [9,10]). However, for failure initiating at or near the FRP/glue/concrete interface, such as interfacial debonding or separation of the concrete cover between the FRP plate and the outermost steel layer (i.e. what is, in the present terminology, referred to as plate peeling), the exact way to obtain the premature failure load is still under debate (e.g. [6]). Such local modes of failure are commonly observed in the experiments (e.g. [11,12]) and are of a largely brittle nature (cf. conventional flexural failure). Indeed, as repeatedly reported in the literature (e.g. [11,12]), tests have demonstrated that even an originally ductile (i.e. under-reinforced) beam subsequently strengthened with FRP will have less ductility than the original beam, provided that plate peeling occurs before the concrete reaches its maximum compressive strain capacity.

The purpose of the present paper is, in the absence of interfacial debonding (at the plate/glue/concrete interface), to identify and investigate the characteristics of all the possible flexural modes of failure which are likely to occur in connection with simply supported reinforced concrete beams upgraded with external FRP plates glued to their soffits. To this end, the effects of variations in the magnitude of Young's modulus of FRP plate (while keeping its associated ultimate tensile strength, for a given beam design, constant) on the potential changes in the flexural ultimate load of R.C. beams with externally bonded FRP plates in the absence and/or presence of plate peeling will be discussed in some detail. Unlike unplated R.C. beams which can either be under-reinforced (ductile) or over-reinforced (brittle), there are, in the absence of interfacial debonding, in general, eight different possible flexural modes of failure for the R.C. beams with external plates, with some of these modes being practically more desirable than others. Using detailed theoretical formulations, it is now possible to determine the particular type of mode of failure associated with each specific FRP plated beam design. Most importantly, closed-form theoretical formulations, which are amenable to simple calculations, have been developed which enable one to determine all the possible critical points of mode changes (i.e. transitions) as a function of variations in the values of FRP plate's Young's modulus (for a given associated ultimate tensile strength), covering the full manufacturing range of these parameters in practice. Full details of the derivations for all the presently reported formulae are given elsewhere [2], with the present paper reporting (in view of space limitations) only the salient features of the proposed method, including the final version of the proposed closed-form theoretical formulae.

2. Background

Theoretically, there are, in the absence of interfacial debonding, eight possible flexural modes of failure for externally plated R.C. beams. This is due to the fact that, in addition to the possibility of the occurrence of plate peeling, there are three elements (namely concrete, internal reinforcement, and external plate) in the plated beams with each of these elements either reaching its failure state or not at the instance of the total failure of the beam. These possible modes of failure are listed as in the following, with the element which controls the final failure in each mode written in italics: (the symbols ***C***, ***R***, and ***P*** refer to Concrete, Rebar, and Plate, respectively).

1. *Crushed concrete*, unyielded bars and unruptured/unyielded plate ***C--***,
2. *Crushed concrete*, unyielded bars and yielded plate ***C–P***,
3. *Crushed concrete*, yielded bars and unruptured/unyielded plate ***CR-***,
4. *Crushed concrete*, yielded bars and plate ***CRP***,
5. Uncrushed concrete, yielded bars and *ruptured FRP plate* ***-RP***,
6. Uncrushed concrete, unyielded bars and *ruptured FRP plate* ***--P***,
7. *Peeled end plate*, uncrushed concrete, yielded bars and unruptured/unyielded plate ***-R-***, and
8. *Peeled end plate*, uncrushed concrete, unyielded bars and unruptured/unyielded plate ***---***.

All such theoretically identified modes of failure for the beams upgraded with either external steel or FRP plates are listed in Table 1 and classified according to the type of bond (full/partial bond capacity). Full bond relates to cases when the beam fails after one or more of the elements of the beam, at the section of maximum bending moment, reaches its ultimate limit while partial bond capacity corresponds to those cases when the beam suffers premature failure due to end plate peeling (which happens away from the maximum bending moment section). As the FRP plates

Table 1
Modes of failure for beams upgraded with external plates

<table>
<tr><th rowspan="2">Capacity</th><th colspan="2">Beam externally reinforced with</th></tr>
<tr><th>FRP plate</th><th>Steel plate</th></tr>
<tr><td>Full bond</td><td colspan="2">***CR-***</td></tr>
<tr><td></td><td></td><td>***CRP***</td></tr>
<tr><td></td><td>***-RP***</td><td></td></tr>
<tr><td></td><td colspan="2">***C--***</td></tr>
<tr><td></td><td></td><td>***C–P***</td></tr>
<tr><td></td><td>***--P***</td><td></td></tr>
<tr><td>Partial bond</td><td colspan="2">***-R-***</td></tr>
<tr><td></td><td colspan="2">---</td></tr>
</table>

and concrete are both brittle, a certain number of the flexural failure modes (namely, ***CRP*** and ***C–P***) which correspond to simultaneous over-straining of both the concrete in compression and the FRP plate in tension, are presently assumed to be extremely unlikely to occur in practice, and have, thus, not been considered when developing the formulations for the FRP plated R.C. beams, as reported in the next section (i.e. Section 3). The underlying reason for this is that these two brittle materials are unlikely to fail together at the same instance, and (most probably) only one of them will (in practice) be the controlling factor as far as the final failure is concerned. It is, however, perhaps worth emphasising that, as indicated in Tables 1 and 2, the occurrence of the ***CRP*** and ***C–P*** modes of failure is certainly a practical possibility in connection with the use of steel plates. The load carrying capacity of the beam will be classified as a partial bond capacity due to premature plate peeling failure, if the concrete in tension within the cover is the controlling factor for the failure mode [13], while it will be classified as full bond capacity if the failure is controlled by either the crushing of concrete or the rupture of FRP plate, at the maximum moment section, with full bond maintained between the FRP plate and concrete up to the final collapse.

Various characteristics of the above failure modes are addressed in some detail in Tables 2 and 3. In particular, Hassanen [2] gives a full account of the general pattern of various changes in the values of individual elements of the plated section with increases in the Young's modulus of the FRP plate, while the ultimate tensile strength for the FRP plate is kept constant: the final outcome is presented in Table 3. It should be noted at once that, in practice, by using a combination of glass and carbon fibres, and adopting an appropriate void ratio, it is, indeed, possible to keep the FRP tensile strength nominally constant and produce unidirectional FRP plates (or sheets) covering a wide range of Young's moduli. In the present work, tension in concrete, below the neutral axis, will be neglected for simplicity, as its effect is (in most cases) of relatively minor importance compared to the other tensile forces in the reinforcing bars and the external plate. For the present purposes, the simply supported beam is assumed to be subjected to symmetrical four-point loading. Following extensive theoretical parametrical studies, as reported fully elsewhere [2], the general patterns of failure modes (for a given associated value of tensile strength for the FRP plate) were found to be as shown in Figs. 2 and 3. Fig. 2 presents a schematic diagram as regards variations of different modes of failure associated with under-reinforced FRP plated R.C. beams, while Fig. 3 presents a similar schematic diagram for over-reinforced FRP plated R.C. beams. In the present terminology, the terms under-reinforced and over-reinforced refer to cases where the successor flexural mode of failure, following the primary mode ***CR-***, will be either ***-RP*** (which is desirable) or ***C--*** (which is brittle), respectively, with the area of the external plate, A_p (amongst other parameters) playing a central role in deter-

Table 2
Various characteristics of the possible flexural modes of failure for FRP – or steel-plated R.C. beams

Mode	Status of section elements			Description of the type of failure
	Concrete	Plate	Tension bars	
C--	$\varepsilon_0 = \varepsilon_m = 0.0035$	$f_p < f_{pu}$ or $f_p < f_y$	$f_s < f_y$	Suddenly, following the crushing of concrete at the top surface of the beam
C–P	$\varepsilon_0 = \varepsilon_m = 0.0035$	$\varepsilon_p > \varepsilon_{py}$ and $f_p = f_{py}$	$f_s < f_y$	Suddenly, following the crushing of concrete at the top surface of the beam
CR-	$\varepsilon_0 = \varepsilon_m = 0.0035$	$f_p < f_{pu}$ or $f_p < f_y$	$\varepsilon_s > \varepsilon_y$ and $f_s = f_y$	After large overall beam curvatures and deformations, associated with propagation of the cracks on the tension side, and subsequent crushing of concrete at the top surface of the beam
CRP	$\varepsilon_0 = \varepsilon_m = 0.0035$	$f_s = f_y$	$\varepsilon_s > \varepsilon_y$	With large overall changes in curvatures and deformations, with the propagation of the cracks within the tension side of the specimen (with the steel plate having yielded), and subsequent crushing of concrete at the top surface of the beam
-RP	$\varepsilon_0 < \varepsilon_m = 0.0035$	$\varepsilon_p = \varepsilon_{pu}$ and $f_p = f_{pu}$	$\varepsilon_s > \varepsilon_y$ and $f_s = f_y$	Following the development of large curvatures and deformations at the tension side of the beam, and after the rupture of FRP. In this mode, the load bearing capacity of the beam is classified as full bond capacity
--P	$\varepsilon_0 < \varepsilon_m = 0.0035$	$\varepsilon_p = \varepsilon_{pu}$ and $f_p = f_{pu}$	$\varepsilon_s < \varepsilon_y$ and $f_s < f_y$	Suddenly, without any prior warning. In this mode, the load bearing capacity of the beam is classified as full bond capacity. It should, however, be noted that this mode will not occur when ductile steel plates are used
-R-	$\varepsilon_0 < 0.0035$	$f_p = \sigma_s$	$\varepsilon_s > \varepsilon_y$ and $f_s > f_y$	Subsequent to the development of large curvatures and deformations at the tension side of the beam, and after the plate with concrete cover have peeled off, as a unit, from underside of the beam, over a portion of the main reinforcing steel located near the end of the plate
---	$\varepsilon_0 < 0.0035$	$f_p = \sigma_s$	$\varepsilon_s < \varepsilon_y$ and $f_s < f_y$	Suddenly, with the concrete cover and plate peeling, as a unit, from the tensile side of the beam

Key to the symbols in Table 2.
f_p, plate tensile axial stress; f_{pu}, FRP plate ultimate tensile strength; f_{py}, yield strength of the steel plate in tension; f_s, axial stress of the tensile bars; f_y, yield strength of the main (embedded) tensile reinforcement; ε_0, maximum concrete strain in compression; ε_m, concrete crushing strain; ε_p, plate tensile axial strain; ε_{pu}, FRP plate ultimate tensile strain; ε_{py}, yield strain of the steel plate in tension; ε_s, axial strain in the tensile bars; ε_y, yield strain of the tensile bars; σ_s, plate tensile axial stress at the instance of plate peeling.

Table 3
Changes in various individual elements of the plated section with increases in the Young's modulus for the FRP plate

Mode	Depth of neutral axis (y)	Effect on section elements												Section flexural capacity
		Concrete in compression			Plate			Bars in tension			Bars in compression			
		Strain	Stress	Total force	Strain (ε_p)	Stress (f_p)	Force (F_p)	Strain (ε_s)	Stress (f_s)	Force (F_s)	Strain (ε'_s)	Stress (f'_s)	Force (F'_s)	
C--	↑	↔	↔	↑	↓	↑	↑	↓	↓	↓	↑	↑	↑	↑
CR-	↑	↔	↔	↑	↓	↑	↑	↓	↔	↔	↑	↑	↑	↑
-RP, ***-R-***	↑	↓	↓	↔	↓	↔	↔	↓	↔	↔	↓	↓	↓	↔
--P,*---*	↑	↓	↓	↓	↓	↔	↔	↓	↓	↓	↓	↓	↓	↓

↑ means increase in magnitude.
↓ means decrease in magnitude.
↔ means no significant change in magnitude.

mining the type of failure mode following ***CR-***: A_p largely determines the appropriate magnitude of the Young's modulus (i.e. whether $E_{(A)}$ or $E_{(C)}$) associated with the critical positions of mode transitions. It should, however, be noted that, throughout the present work, the unplated (original) beam is assumed to be under-reinforced. It is perhaps worth mentioning that, unlike unplated R.C. beams (which can either be ductile if under-reinforced or brittle if over-reinforced), even when at the instance of failure of the beam the internal steel bars have yielded and the external FRP plate has ruptured, the final failure is not fully ductile [14]. Following the yielding of the bars, it is noted that the subsequent portion of the overall load-central deflection curve is of an ascending type up until total sudden collapse as a result of the brittle FRP plate rupture. Despite this potential shortcoming of FRP plated beams (i.e. their lack of full ductility at failure), it is suggested that the ***-RP*** mode of failure (associated with which there is a full utilisation of the ultimate tensile strengths of both the embedded steel bars and the brittle FRP plate) is, indeed, the most desirable (although not fully ductile) mode of failure (amongst all the presently considered eight flexural failure modes associated with FRP plated R.C. beams).

3. Determination of the critical FRP elastic moduli

Depending on whether the final mode of failure involves occurrence of plate peeling (case B) or not (case A), closed-form formulae have been developed for determining the variations in the flexural modes of failure for a FRP plated beam associated with changes in the magnitude of Young's modulus for the FRP material (while keeping its associated ultimate tensile strength constant). As mentioned previously, detailed derivations of the formulations for determining the critical values of moduli of elasticity for FRP plates, at which changes in the failure modes are initiated, are given elsewhere [2]. For the present purposes, in view of space limitations, only the final formulae are given in order to enable the interested reader to better understand (and appreciate) the resulting numerical data as presented in Section 4. Very briefly, according to the newly proposed method, the following steps should be followed (in conjunction with Figs. 2 and 3), for determining these critical values of plate moduli of elasticity, for the FRP plated beam cross-section in Fig. 1. It should be noted that in the following steps, the maximum concrete strain in compression $\varepsilon_0 = 0.0035$ unless stated otherwise, and in Figs 2 and 3, as regards the parameter $\boldsymbol{E}$, the lower case subscripts refer to the partial bond behaviour while the upper case subscripts refer to the full bond behaviour.

3.1. Case A

This case relates to those instances when either the plate peeling stress is higher than the ultimate tensile strength of the plate, or there are certain design arrangements which

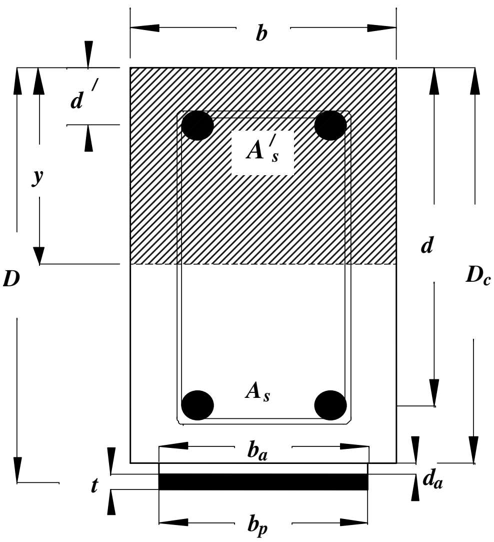

Fig. 1. Details of plated R.C. beam cross-section.

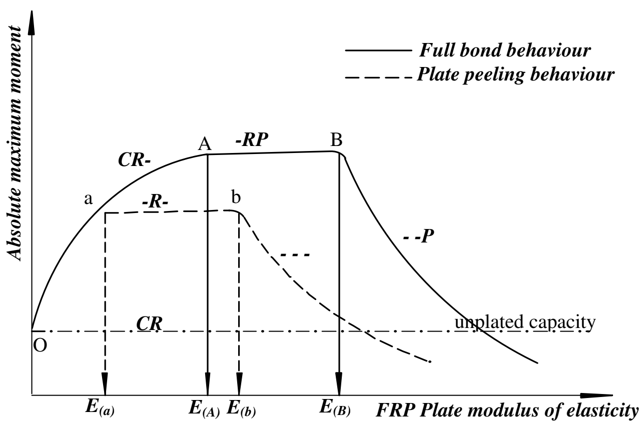

Fig. 2. Modes of failure for under-reinforced plated beam.

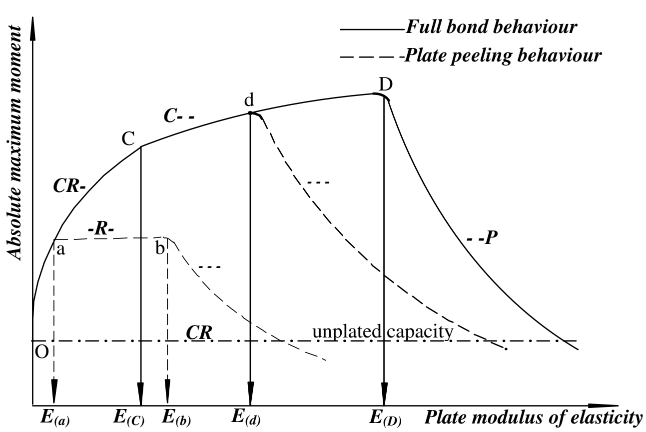

Fig. 3. Modes of failure for over-reinforced plated beam.

ensure that the plate peeling will not happen (such as presence of effective plate end anchorages) – under such conditions, then:

1. Calculate $\boldsymbol{y}_{\mathrm{A}}$ and $\boldsymbol{E}_{(\mathrm{A})}$ from the following:

$$y_{\mathrm{A}}^2 b\left(\frac{\beta}{\varepsilon_0}\right)\left[\frac{E_{\mathrm{c}}\beta}{6}+0.67f_{\mathrm{cu}}\left(\frac{\varepsilon_0}{\beta}-\frac{2}{3}\right)\right] + y_{\mathrm{A}}(A_{\mathrm{s}}'E_{\mathrm{s}}\varepsilon_0 - A_{\mathrm{s}}f_{\mathrm{y}} - A_{\mathrm{p}}f_{\mathrm{pu}}) - A_{\mathrm{s}}'E_{\mathrm{s}}\varepsilon_0 d' = 0 \quad (1)$$

where, E_{c} = modulus of elasticity for concrete, E_{s} = Young's modulus for the steel bars, A_{s} = total cross-section area of tensile bars, A_{s}' =total cross-section area of compression bars, β = concrete compressive strain at the onset of peak stress ($= 2.44 \times 10^{-4}\sqrt{f_{\mathrm{cu}}}$, where f_{cu} = concrete cube crushing strength in MPa [15]), A_{p} = FRP plate cross-sectional area, $\varepsilon_{\mathrm{pu}}$ = ultimate tensile strain in the FRP plate, f_{pu} = ultimate tensile strength of the FRP plate, and y = depth of neutral axis with its subscript denoting the associated critical mode transition point. The other terms are defined in Fig. 1, and for fairly linear behaviour of the FRP material up until tensile failure:

$$E_{(\mathrm{A})} = \frac{f_{\mathrm{pu}}}{\varepsilon_{\mathrm{pu}}} = \frac{f_{\mathrm{pu}}}{0.0035}\frac{y_{\mathrm{A}}}{(D-y_{\mathrm{A}})} \quad (2)$$

Alternatively, if the influence of the embedded steel bars in the compression side is ignored, and the simplified stress block for concrete as that recommended by BS8110 [15] is assumed, rather than using Eqs. (1) and (2), one may use the following simpler versions:

$$A_{\mathrm{s}}f_{\mathrm{y}} + A_{\mathrm{p}}f_{\mathrm{pu}} = 0.9y_{\mathrm{A}}b \times 0.67f_{\mathrm{cu}} \quad (3)$$

or

$$y_{\mathrm{A}} = \frac{A_{\mathrm{s}}f_{\mathrm{y}} + A_{\mathrm{p}}f_{\mathrm{pu}}}{0.67f_{\mathrm{cu}}0.9b} \quad (4)$$

The critical value of the plate modulus of elasticity, $\boldsymbol{E}_{(\mathrm{A})}$, may, then, be determined by a very simple closed-form relationship:

$$E_{(\mathrm{A})} = \frac{f_{\mathrm{pu}}}{\varepsilon_{\mathrm{pu}}} = \frac{f_{\mathrm{pu}}(A_{\mathrm{s}}f_{\mathrm{y}} + A_{\mathrm{p}}f_{\mathrm{pu}})}{0.0035(0.9\times 0.67f_{\mathrm{cu}}bD - A_{\mathrm{s}}f_{\mathrm{y}} - A_{\mathrm{p}}f_{\mathrm{pu}})} \quad (5)$$

2. Calculate $\boldsymbol{y}_{\mathrm{C}}$ and $\boldsymbol{E}_{(\mathrm{C})}$ from the following:

$$y_{\mathrm{C}} = \frac{\varepsilon_0 d}{(\varepsilon_0 + \frac{f_{\mathrm{y}}}{E_{\mathrm{s}}})} \quad (6)$$

$$E_{(\mathrm{C})} = \frac{A_{\mathrm{s}}'E_{\mathrm{s}}\varepsilon_0\left(1-\frac{d'}{y_{\mathrm{C}}}\right) + y_{\mathrm{C}}b\left(\frac{\beta}{\varepsilon_0}\right)\left[\frac{E_{\mathrm{c}}\beta}{6}+0.67f_{\mathrm{cu}}\left(\frac{\varepsilon_0}{\beta}-\frac{2}{3}\right)\right] - A_{\mathrm{s}}f_{\mathrm{y}}}{A_{\mathrm{p}}\left(\frac{D}{y_{\mathrm{C}}}-1\right)\varepsilon_0} \quad (7)$$

3. If $\boldsymbol{E}_{(\mathrm{C})} < \boldsymbol{E}_{(\mathrm{A})}$, then, the plated beam is an over-reinforced type, and the next mode of failure, following the primary mode ***CR-***, will be the brittle one ***C--***; being initiated at the critical plate modulus of elasticity $\boldsymbol{E}_{(\mathrm{C})}$.
4. If $\boldsymbol{E}_{(\mathrm{C})} > \boldsymbol{E}_{(\mathrm{A})}$, then, the plated beam is of an under-reinforced type, and the subsequent mode of failure, following the primary mode ***CR-***, will be the desirable ***–RP*** type; being initiated at the critical value of plate modulus of elasticity $\boldsymbol{E}_{(\mathrm{A})}$.

5. For an over-reinforced plated beam (i.e. the beam with $\boldsymbol{E}_{(\mathrm{C})} < \boldsymbol{E}_{(\mathrm{A})}$), calculate $\boldsymbol{y}_{\mathrm{D}}$ and $\boldsymbol{E}_{(\mathrm{D})}$ from the following:

$$y_{\mathrm{D}}^2\left[\frac{E_{\mathrm{c}}\beta}{6}+0.67f_{\mathrm{cu}}\left(\frac{\varepsilon_0}{\beta}-\frac{2}{3}\right)\right]b\left(\frac{\beta}{\varepsilon_0}\right) + y_{\mathrm{D}}[E_s\varepsilon_0(A_{\mathrm{s}}+A'_{\mathrm{s}})-A_{\mathrm{p}}f_{\mathrm{pu}}] - E_{\mathrm{s}}\varepsilon_0(A'_{\mathrm{s}}d'+A_{\mathrm{s}}d)=0 \tag{8}$$

$$E_{(\mathrm{D})}=\frac{f_{\mathrm{pu}}}{\varepsilon_{\mathrm{pu}}}=\frac{f_{\mathrm{pu}}}{0.0035}\frac{y_{\mathrm{D}}}{(D-y_{\mathrm{D}})} \tag{9}$$

6. For an under-reinforced plated beam (i.e. the beam with $\boldsymbol{E}_{(\mathrm{C})} > \boldsymbol{E}_{(\mathrm{A})}$), on the other hand, calculate $\boldsymbol{y}_{\mathrm{B}}$ and ε_0 from the following:

$$y_{\mathrm{B}}^2[K_3-K'-K_{\mathrm{f}}]+y_{\mathrm{B}}[d(K'+K_{\mathrm{f}}-2K_3)+K'd'+K_{\mathrm{T}}] + d[K_3d-K'd'-K_T]=0 \tag{10}$$

and

$$\varepsilon_0=\varepsilon_{\mathrm{y}}\frac{y_{\mathrm{B}}}{d-y_{\mathrm{B}}} \tag{11}$$

where

$$K_1=\frac{0.67f_{\mathrm{cu}}-E_{\mathrm{c}}\beta}{\beta^2},\quad K_3=\left[\frac{bE_{\mathrm{c}}}{2}\frac{\beta^2}{\varepsilon_{\mathrm{s}}}+\frac{bK_1}{3}\frac{\beta^3}{\varepsilon_{\mathrm{s}}}-0.67f_{\mathrm{cu}}b\frac{\beta}{\varepsilon_{\mathrm{s}}}\right],$$

$K_{\mathrm{f}}=0.67f_{\mathrm{cu}}by, K'=A'_{\mathrm{s}}E_{\mathrm{s}}\varepsilon_{\mathrm{s}}$,
and $K_{\mathrm{T}}=(A_{\mathrm{s}}f_{\mathrm{y}}+A_{\mathrm{p}}f_{\mathrm{pu}})$

where, ε_{s} = axial strain in the tensile bars.

7. If $\boldsymbol{\varepsilon}_0 < \beta$, then, $\boldsymbol{y}_{\mathrm{B}}$ should be recalculated by using:

$$y_{\mathrm{B}}^3[K_2-K_{\mathrm{E}}]+y_{\mathrm{B}}^2[K_{\mathrm{E}}d-K'-K_{\mathrm{T}}] + y_{\mathrm{B}}[K'(d+d')+2K_{\mathrm{T}}d]-(K'dd'+K_{\mathrm{T}}d^2)=0 \tag{12}$$

where

$$K_2=\frac{bK_1\varepsilon_{\mathrm{s}}^2}{3}\quad\text{and}\quad K_{\mathrm{E}}=\frac{bE_{\mathrm{c}}\varepsilon_{\mathrm{s}}}{2}$$

8. Finally, $\boldsymbol{E}_{(\mathrm{B})}$ is given by:

$$E_{(\mathrm{B})}=\frac{f_{\mathrm{pu}}}{\varepsilon_{\mathrm{pu}}}=\frac{(d-y_{\mathrm{B}})}{(D-y_{\mathrm{B}})}\frac{f_{\mathrm{pu}}}{f_{\mathrm{y}}}E_{\mathrm{s}} \tag{13}$$

3.2. Case B

This case relates to those instances when the plate peeling stress is found to be lower than the plate ultimate tensile strength, and the beam experiences premature plate peeling- under such conditions, the type of behaviour (i.e. the corresponding changes in the flexural failure modes) and the critical values of moduli of elasticity for the plate may be determined as follows:

1. Calculate $\boldsymbol{y}_{\mathrm{a}}$ and $\boldsymbol{E}_{(\mathrm{a})}$, using:

$$y_{\mathrm{a}}^2b\left(\frac{\beta}{\varepsilon_0}\right)\left[\frac{E_{\mathrm{c}}\beta}{6}+0.67f_{\mathrm{cu}}\left(\frac{\varepsilon_0}{\beta}-\frac{2}{3}\right)\right] + y_{\mathrm{a}}(A'_{\mathrm{s}}E_{\mathrm{s}}\varepsilon_0-A_{\mathrm{s}}f_{\mathrm{y}}-A_{\mathrm{p}}\sigma_{\mathrm{s}})-A'_{\mathrm{s}}E_{\mathrm{s}}\varepsilon_0d'=0 \tag{14}$$

$$E_{(\mathrm{a})}=\frac{\sigma_{\mathrm{s}}}{\varepsilon_{\mathrm{pel}}}=\frac{\sigma_{\mathrm{s}}}{0.0035}\frac{y_{\mathrm{a}}}{(D-y_{\mathrm{a}})} \tag{15}$$

where, $\varepsilon_{\mathrm{pel}}$ = plate tensile axial strain associated with σ_{s}, and σ_{s} = plate longitudinal tensile stress at the instance of plate peeling failure. As fully explained elsewhere [13], the magnitude of σ_{s} depends on the spacings of flexural cracks within the concrete cover, and due to the random spacings of flexural cracks in practice (which can vary by a factor of, say, 2), the magnitude of σ_{s} is not unique: σ_{s} lies within the range $\sigma_{\mathrm{s(min)}} < \sigma_{\mathrm{s}} < \sigma_{\mathrm{s(max)}}$. Ref. [13] gives the closed-form formulae for calculating both $\sigma_{\mathrm{s(min)}}$ and $\sigma_{\mathrm{s(max)}}$, with these lower and upper limiting values for σ_{s} being the ones to be substituted for σ_{s} throughout this paper, in order to cover both (i.e. lower and upper) bounding solutions in Eqs. (14) and (15) as well as the other (relevant) equations throughout the present paper.

2. Calculate $\boldsymbol{y}_{\mathrm{d}}$ and $\boldsymbol{E}_{(\mathrm{d})}$ from:

$$y_{\mathrm{d}}^2\left[\frac{E_{\mathrm{c}}\beta}{6}+0.67f_{\mathrm{cu}}\left(\frac{\varepsilon_0}{\beta}-\frac{2}{3}\right)\right]b\left(\frac{\beta}{\varepsilon_0}\right)+y_{\mathrm{d}}[E_{\mathrm{s}}\varepsilon_0(A_{\mathrm{s}}+A'_{\mathrm{s}})-A_{\mathrm{p}}\sigma_{\mathrm{s}}] - E_{\mathrm{s}}\varepsilon_0(A'_{\mathrm{s}}d'+A_{\mathrm{s}}d)=0 \tag{16}$$

$$E_{(\mathrm{d})}=\frac{\sigma_{\mathrm{s}}}{\varepsilon_{\mathrm{pel}}}=\frac{\sigma_{\mathrm{s}}}{0.0035}\frac{y_{\mathrm{d}}}{(D-y_{\mathrm{d}})} \tag{17}$$

3. If $\boldsymbol{E}_{(\mathrm{d})} > \boldsymbol{E}_{(\mathrm{a})}$, then, the plated beam is categorised as an under-reinforced one, and the subsequent mode of failure, following the primary mode ***CR-***, will be the ***-R***-type; being initiated at the critical value of plate modulus of elasticity $\boldsymbol{E}_{(\mathrm{a})}$. For such a beam, the brittle failure mode ---, then, initiates at the critical value of plate modulus of elasticity $\boldsymbol{E}_{(\mathrm{b})}$, which may be predicted as follows:

$$y_{\mathrm{b}}^2[K_3-K'-K_{\mathrm{f}}]+y_{\mathrm{b}}[d(K'+K_{\mathrm{f}}-2K_3)+K'd'+K_{\mathrm{T}}] + d[K_3d-K'd'-K_{\mathrm{T}}]=0 \tag{18}$$

where, $K_{\mathrm{T}}=(A_{\mathrm{s}}f_{\mathrm{y}}+A_{\mathrm{p}}\sigma_{\mathrm{s}})$, and K', K_{f}, K_1, and K_3 are as defined previously, with

$$\varepsilon_0=\varepsilon_{\mathrm{y}}\frac{y_{\mathrm{b}}}{d-y_{\mathrm{b}}} \tag{19}$$

4. If $\varepsilon_0 < \beta$, $\boldsymbol{y}_{\mathrm{b}}$ should be recalculated by using:

$$y_{\mathrm{b}}^3[K_2-K_{\mathrm{E}}]+y_{\mathrm{b}}^2[K_{\mathrm{E}}d-K'-K_{\mathrm{T}}] + y_{\mathrm{b}}[K'(d+d')+2K_{\mathrm{T}}d]-(K'dd'+K_{\mathrm{T}}d^2)=0 \tag{20}$$

where, K_2, and K_{E} are as defined previously.

5. Finally, $\boldsymbol{E}_{(\mathrm{b})}$ is predicted from

$$E_{(\mathrm{b})}=\frac{\sigma_{\mathrm{s}}}{\varepsilon_{\mathrm{pel}}}=\frac{(d-y_{\mathrm{b}})}{(D-y_{\mathrm{b}})}\frac{\sigma_{\mathrm{s}}}{f_{\mathrm{y}}}E_{\mathrm{s}} \tag{21}$$

6. If $\boldsymbol{E}_{(\mathrm{d})} < \boldsymbol{E}_{(\mathrm{a})}$, then, the plated beam will behave as an over-reinforced one, and the brittle mode --- will follow, initiated at the critical value of plate modulus of elasticity $\boldsymbol{E}_{(\mathrm{d})}$.

4. Verification of the proposed formulae for the critical values of E_P for the FRP plate

In this section, the proposed closed-form formulae for determining the critical values of plate moduli of elasticity,

E_p, associated with various failure modes, will be checked against results based on numerical (i.e. theoretical) parametric studies, using the same group of twenty one beam designs which have been used in the theoretical parametric studies as discussed by Hassanen [2].

In Table 4, the numerical results relating to the predicted values of $\boldsymbol{E}_{(A)}$, $\boldsymbol{E}_{(B)}$, $\boldsymbol{E}_{(C)}$ and $\boldsymbol{E}_{(D)}$ associated with the full bond behaviour are compared with the critical values based on the numerical parametric studies [2], where the changes in the failure modes (for a given beam design) with increasing values of the plate moduli of elasticity (while keeping the associated ultimate tensile strength for the FRP material, constant) have been fully reported. Tables 5 and 6 show similar comparisons for the upper and lower bound peeling moments, respectively, for the corresponding partially bonded behaviour, and present a comparison of the values of $\boldsymbol{E}_{(a)}$, $\boldsymbol{E}_{(b)}$ and $\boldsymbol{E}_{(d)}$ based on the closed-form formulae (as presented in the previous section) with the corresponding critical values as obtained from the numerical parametric studies [2]. It is, perhaps, worth mentioning that the beam reference numbers given in Tables 4–6 are the same as those used in the references from which the specific beam design details were obtained by Hassanen [2], with full details of all these references given elsewhere [2].

In these tables, the predicted second mode of failure (as the successor to the primary mode ***CR-***) is shown in column (3), and is determined according to the lower value of $\boldsymbol{E}_{(A)}$ (column (1)) and $\boldsymbol{E}_{(C)}$ (column (2)) in Table 4, or the lower value of $\boldsymbol{E}_{(a)}$ (column (1)) and $\boldsymbol{E}_{(C)}$ (column (2)) in Tables 5 and 6. If $\boldsymbol{E}_{(C)}$ is the lower value, then, the predicted second mode of failure will be the ***C--*** mode associated with ORS (over-reinforced section) state of $\boldsymbol{E}_{(B)}$ in column (4) – i.e. according to Fig. 3, $\boldsymbol{E}_{(B)}$ is not applicable. The same holds true for $\boldsymbol{E}_{(b)}$ which corresponds to the partial bond behaviour, as in Tables 5 and 6: for the ***C--*** mode, $\boldsymbol{E}_{(b)}$ is not applicable because the section is classified as an over-reinforced one – see Fig. 3. On the other hand, if $\boldsymbol{E}_{(C)}$ is the higher value, then, the predicted second mode of failure in column (3) is either the ***--RP*** mode (corresponding to $\boldsymbol{E}_{(A)}$ for full bond behaviour in Table 4) or the ***-R-*** mode (corresponding to $\boldsymbol{E}_{(a)}$ for partial bond behaviour in Tables 5 and 6). In such a case, the critical value $\boldsymbol{E}_{(D)}$ or $\boldsymbol{E}_{(d)}$ in column (5) is not applicable as the section is classified as an under-reinforced one – see Fig. 2.

In Table 4, the predicted second mode of failure in column (3) should be compared with that resulting from the numerical parametric studies as given in column (7). Because the numerical parametric studies were carried out with an interval of 10 GPa for the plate modulus of elasticity, the exact critical value is not available, and only the range over which the mode change-over happens (e.g. 140–150 GPa) is shown. Similar results, for the partial bond behaviour, are shown in Tables 5 and 6. In Tables 4–6, the lower value (as predicted by the proposed closed-form formulae), of those given in columns (1) and (2) should be compared with the corresponding numerically based result in column (6). Finally, in Tables 4–6, the predicted value, based on the closed-form formulae,

Table 4
Critical values of $\boldsymbol{E}_p$ and modes of failure (full bond behaviour)

Beam	Predicted					Numerical parametric study (10 GPa intervals for E_p)		
	$E_{(A)}$ GPa (1)	$E_{(C)}$ GPa (2)	Second mode of failure (3)	$E_{(B)}$ GPa (4)	$E_{(D)}$ GPa (5)	$E_{(A)}$ or $E_{(C)}$ GPa (6)[a]	Second mode of failure (7)	$E_{(B)}$ or $E_{(D)}$ GPa (8)[a]
H-A1b	149	594	***-RP***	368	URS	150–160	***-RP***	200+
H-A2g	262	382	***-RP***	342	URS	200+	***NA***	200+
H-B6	161	478	***-RP***	335	URS	170–180	***-RP***	200+
H-B9	161	478	***-RP***	335	URS	170–180	***-RP***	200+
H-2Cu	119	1082	***-RP***	448	URS	120–130	***-RP***	200+
H-2Ca	119	1082	***-RP***	448	URS	120–130	***-RP***	200+
CC	26	427	***-RP***	143	URS	20–30	***-RP***	140–150
AA	77	234	***-RP***	135	URS	80–90	***-RP***	130–140
BB	51	312	***-RP***	138	URS	50–60	***-RP***	130–140
DD	51	312	***-RP***	138	URS	50–60	***-RP***	130–140
C	10	210	***-RP***	56	URS	10–20	***-RP***	50–60
F	18	104	***-RP***	54	URS	10–20	***-RP***	50–60
H	36	117	***-RP***	79	URS	30–40	***-RP***	70–80
J	83	313	***-RP***	196	URS	80–90	***-RP***	190–200
L	41	785	***-RP***	217	URS	40–50	***-RP***	200+
N	−7840	156	***C--***	ORS	5047	140–150	***C--***	200+
F-P1	10	506	***-RP***	50	URS	10–20	***-RP***	40–50
F-P2	12	252	***-RP***	49	URS	10–20	***-RP***	40–50
F-P2B	12	252	***-RP***	49	URS	10–20	***-RP***	40–50
F-P2BW	12	252	***-RP***	49	URS	10–20	***-RP***	40–50
F-P3J	14	167	***-RP***	48	URS	10–20	***-RP***	40–50

Notes. URS, Under-reinforced section: $\boldsymbol{E}_{(D)}$ is not applicable (Fig. 2); ORS, Over-reinforced section: $\boldsymbol{E}_{(B)}$ is not applicable (Fig. 3); 200+, Value higher than the maximum of the studied range (i.e. higher than 200 GPa); ***NA***, Not available.

[a] n–$(n+10)$ = Critical value of $\boldsymbol{E}_p$ (where the mode is changed) lies between n and $(n+10)$ GPa.

Table 5
Critical values of E_p and modes of failure (partial bond behaviour: $\sigma_s = \sigma_{s(max)}$)

Beam	Predicted					Numerical parametric study (10 GPa intervals for E_p)		
	$E_{(a)}$ GPa (1)	$E_{(C)}$ GPa (2)	Second mode of failure (3)	$E_{(b)}$ GPa (4)	$E_{(d)}$ GPa (5)	$E_{(a)}$ or $E_{(C)}$ GPa (6)[a]	Second mode of failure (7)	$E_{(b)}$ or $E_{(d)}$ GPa (8)[a]
H-A1b	62	594	***-R-***	235	URS	60–70	*-R-*	200+
H-A2g	22	382	***-R-***	121	URS	20–30	***-R-***	100–110
H-B6	60	478	***-R-***	203	URS	60–70	***-R-***	200+
H-B9	60	478	*-R-*	203	URS	60–70	***-R-***	200+
H-2Cu	85	1082	***-R-***	364	URS	80–90	***-R-***	200+
H-2Ca	85	1082	***-R-***	364	URS	80–90	***-R-***	200+
CC	10	427	***-R-***	81	URS	10–20	***-R-***	80–90
AA	11	234	***-R-***	33	URS	10–20	***-R-***	30–37.2
BB	12	312	***-R-***	51	URS	10–20	***-R–***	50–60
DD	12	312	***-R-***	51	URS	10–20	***-R-***	50–60
C	7	210	***-R-***	46	URS	0–10	***-R-***	40–50
F	4	104	***-R-***	22	URS	0–10	***-R-***	20–30
H	4	117	***-R-***	23	URS	0–10	***-R-***	20.7–30
J	11	313	***-R-***	65	URS	10–20	***-R-***	60–70
L	28	785	***-R-***	169	URS	20–30	***-R-***	160–170
N	5	156	***-R-***	25	URS	0–10	***-R-***	30–40
F-P1	12	506	***-RP*** ↑	50	URS	10–20	***-RP*** ↑	40–50
F-P2	12	252	***-RP*** ↑	49	URS	10–20	***-RP*** ↑	40–50
F-P2B	12	252	***-RP*** ↑	49	URS	10–20	***-RP*** ↑	40–50
F-P2BW	12	252	***-RP*** ↑	49	URS	10–20	***-RP*** ↑	40–50
F-P3J	14	167	***-RP*** ↑	48	URS	10–20	***-RP*** ↑	40–50

Notes. URS, Under-reinforced section: $\boldsymbol{E}_{(d)}$ is not applicable (Fig. 2); 200+, Value higher than the maximum of the studied range (i.e. higher than 200 GPa); ↑, $\sigma_{s(max)}$ is higher than the ultimate strength of the plate (full bond behaviour), where $\sigma_{s(max)}$ = upper bound to the magnitude of plate longitudinal tensile stress at the instance of plate peeling failure [13].

[a] n–($n + 10$) = Critical value of $\boldsymbol{E}_p$ (where the mode is changed) lies between n and ($n + 10$) GPa.

Table 6
Critical values of E_p and modes of failure (partial bond behaviour: $\sigma_s = \sigma_{s(min)}$)

Beam	Predicted					Numerical parametric study (10 GPa intervals for E_p)		
	$E_{(a)}$ GPa (1)	$E_{(C)}$ GPa (2)	Second mode of failure (3)	$E_{(b)}$ GPa (4)	$E_{(d)}$ GPa (5)	$E_{(a)}$ or $E_{(C)}$ GPa (6)[a]	Second mode of failure (7)	$\boldsymbol{E}_{(b)}$ or $\boldsymbol{E}_{(d)}$ GPa (8)[a]
H-A1b	21	594	***-R-***	117	URS	20–30	***-R-***	120–130
H-A2g	9	382	***-R-***	60	URS	0–10	***-R-***	50–60
H-B6	20	478	***-R-***	101	URS	20–30	***-R-***	100–110
H-B9	20	478	***-R-***	101	URS	20–30	***-R-***	100–110
H-2Cu	31	1082	***-R-***	182	URS	30–40	***-R-***	180–190
H-2Ca	31	1082	***-R-***	182	URS	30–40	***-R-***	180–190
CC	4	427	***-R-***	41	URS	0–10	***-R-***	40–50
AA	5	234	***-R-***	16	URS	0–10	***-R-***	10–20
BB	5	312	***-R-***	26	URS	0–10	***-R-***	20–30
DD	5	312	***-R-***	26	URS	0–10	***-R-***	20–30
C	3	210	***-R-***	23	URS	0–10	***-R-***	20–30
F	1	104	***-R-***	11	URS	0–10	***-R-***	0–11.7
H	1	117	***-R-***	11	URS	0–10	***-R-***	10–20
J	4	313	***-R-***	32	URS	0–10	***-R-***	30.3–40
L	10	785	***-R-***	*85*	URS	10–20	***-R-***	80–90
N	2	156	***-R-***	12	URS	0–10	***-R-***	10–20
F-P1	10	506	***-RP*** ↑	50	URS	10–20	***-RP*** ↑	40–50
F-P2	12	252	***-RP*** ↑	49	URS	10–20	***-RP*** ↑	40–50
F-P2B	12	252	***-RP*** ↑	49	URS	10–20	***-RP*** ↑	40–50
F-P2BW	12	252	***-RP*** ↑	49	URS	10–20	***-RP*** ↑	40–50
F-P3J	14	167	***-RP*** ↑	48	URS	10–20	***-RP*** ↑	40–50

Notes. URS, Under-Reinforced Section: $\boldsymbol{E}_{(d)}$ is not applicable (Fig. 3); 200+, Value higher than the maximum of the studied range (i.e. higher than 200 GPa); ↑, $\sigma_{s(min)}$ is higher than the ultimate strength of the plate (full bond behaviour), where $\sigma_{s(min)}$ = lower bound to the magnitude of plate longitudinal tensile stress at the instance of plate peeling failure [13].

[a] n–($n + 10$) = Critical value of $\boldsymbol{E}_p$ (where the mode is changed) lies between n and ($n + 10$) GPa.

in columns (4) or (5) (whichever is applicable) should be compared with the corresponding numerically based result in column (8).

A careful examination of such results strongly suggest that the proposed closed-form formulae successfully predict the critical values for the moduli of elasticity associated with the failure mode transition points, although (in some cases) certain results may not be compared because the numerical parametric studies were carried out covering a limited (but practical) range of moduli of elasticity for FRP ($10 < \boldsymbol{E}_\mathrm{p} < 200$ GPa) which do not cover the whole range of values for this parameter as is predictable using the closed-form solutions. For certain cases, such closed-form solutions predict values of the critical moduli of elasticity as high as 5047 GPa: such values are outside the current manufacturing limits for FRP materials and are of not much practical concern. In other words, such extreme changes of failure modes for certain beam designs (although theoretically possible) do not happen in practice. It should also be noted that for beam N in Table 4, $\boldsymbol{E}_{(\mathrm{A})}$ has a negative value: the reason for this is that, unlike all the other beams in Table 4, beam N is an over-reinforced one even in its unplated condition so that, for even vanishingly small values of FRP modulus, its mode of failure in Fig. 2 is not ***CR-***. As mentioned previously, all the presently proposed formulae are based on the assumption that in their unplated condition the beams are under-reinforced, with the beam N being included in these tables in order to demonstrate this point.

Finally, although the results presented in Tables 4–6 provide encouraging support for the predictions based on the proposed closed-form formulae relating to the critical values of the plate moduli of elasticity (for a constant associated ultimate tensile strength for the FRP plate, in a given beam design), admittedly the comparisons in these Tables are with the results of other calculations, and not with test data. It is, however, noteworthy that in the references from which the beam designs in Tables 4–6 were obtained, for each given beam design, an experimentally obtained failure load and associated mode of failure is reported, with the very encouraging correlations between such test data and the predictions based on similar numerical studies (i.e. as those adopted in Tables 4–6) reported elsewhere [2].

5. Discussion

Although, at first sight, it may appear that the present paper merely reports a menu of formulas, based on a series of well-known solutions to an aspect of the flexural analysis of R.C. beams that easily lends itself to the kind of closed-form solutions presented by the authors, it should be noted at once that, as it is sometimes the case, appearances can be deceptive and the main point of the present paper is that the elastic modulus of FRP plates can be adjusted and that such changes in the FRP elastic modulus can significantly affect the failure mode of beams strengthened with the FRP. This is believed to be a practically important point which has not been even touched upon (in a quantitative way) in the previously available extensive in the literature on FRP plated R.C. beams. In particular, it is perhaps worth mentioning that in later work by Heathcote [8], the work reported in the present paper has been used as a basis for developing a simple design procedure for FRP plated R.C. beams, using which one can determine the appropriate values of both the ultimate tensile strength and the elastic modulus for the FRP plate so that the plated beam would not suffer from undesirable premature plate peeling failure, and that its associated ultimate moment capacity would be $\boldsymbol{M}_{\boldsymbol{\text{-}RP}}$ (i.e. that associated with the desirable ***-RP*** mode of failure). Moreover, unlike the present work which has assumed the absence of any local interfacial debonding, Heathcote [8] has developed a simple method (which is backed by extensive large scale test data) for predicting the occurrence of interfacial debonding (at the FRP/glue/concrete interface) the associated maximum bending moment of which is $\boldsymbol{M}_\mathrm{theo}$, with the lower of $\boldsymbol{M}_\mathrm{theo}$ and $\boldsymbol{M}_{\boldsymbol{\text{-}RP}}$ then suggested to be the critical one for design purposes. In other words, the presently reported work constitutes only part of what has been achieved to date, and further developments of this work are so extensive that they need to be reported in future publications.

6. Conclusions

In the absence of interfacial debonding, a detailed classification of all the possible flexural modes of failure in connection with FRP plated R.C. beams is reported, with a quantitative treatment of the variations in the failure modes as a function of changes in the FRP Young's modulus (for a constant associated ultimate tensile strength for the FRP plate, in a given beam design), covering the full range of manufacturing limits for the FRP material. The proposed formulations are amenable to simple calculations, which is of value to practising engineers.

References

[1] Hollaway LC, Leeming MB, editors. Strengthening of reinforced concrete structures using externally-bonded FRP composites in structural and civil engineering. Cambridge, England: Woodhead Publishing Limited; 1999.

[2] Hassanen MAH. Behaviour of R.C. beams upgraded with externally bonded steel or FRP plates. PhD Thesis, Loughborough University, UK, 2000.

[3] Teng JG, Chen JF, Smith ST, Lam L. FRP strengthened RC structures. UK: John Wiley and Sons; 2002.

[4] Leung CKY. FRP debonding from a concrete substrate: some recent findings against conventional belief. Cement and Concrete Composites 2006;28:742–8.

[5] Lu XZ, Teng JG, Ye LP, Jiang JJ. Bond-slip models for FRP sheets/plates bonded to concrete. Eng Struct 2005;27:920–37.

[6] Gao B, Leung CKY, Kim JK. Prediction of concrete cover separation failure for RC beams strengthened with CFRP strips. Eng Struct 2005;27:177–89.

[7] Teng JG, Chen JF, Smith ST, Lam L. Behaviour and strength of FRP-strengthened RC structures.: a state-of-the-art review. Proceed-

ings of the Institution of Civil Engineers, Structures and Buildings 2003;156(1):51–62.
[8] Heathcote PM. Theoretical and experimental study on FRP or steel plated R.C. beams. PhD Thesis, Loughborough University, UK, 2004.
[9] An W, Saadatmanesh H, Ehsani MR. RC beams strengthened with FRP plates, II: analysis and parametric study. J Struct Eng ASCE 1991;117(11):3434–55.
[10] Triantafillou TC, Plevris N. Strengthening of RC beams with epoxy-bonded fibre-composite materials. Mater Struct 1992;25(25):201–11.
[11] Saadatmanesh H, Ehsani MR. RC beams strengthened with GFRP Plates, I: experimental study. J Struct Eng ASCE 1991;117(11): 3417–33.
[12] Meier U, Deuring M, Meier H, Schwegler G. Strengthening of structures with CFRP laminates: research and applications in Switzerland. Advanced Composite Materials in Bridges and Structures, Canadian Society for Civil Engineering, Canada 1992: 243–51.
[13] Raoof M, Hassanen MAH. Peeling failure of R.C. beams with FRP or steel plates glued to their soffits. Proceedings of the Institution of Civil Engineers, Structures and Buildings 2000; 140(August):291–305.
[14] Arduini M, Di Tommaso A, Nanni A. Brittle failure in FRP plate and sheet bonded beams. ACI Struct J 1997;94(4):363–70.
[15] BS8110, Structural Use of Concrete - British Standards Institute BSI 1997.